

**19th International Conference on  
Harmonisation within Atmospheric Dispersion Modelling for Regulatory Purposes  
3-6 June 2019, Bruges, Belgium**

---

**EVALUATION OF ANSYS-FLUENT MODEL AGAINST FIELD DATA IN THE  
FRAMEWORK OF THE VIEPI PROJECT**

*Annalisa Di Bernardino<sup>1</sup>, Agnese Pini<sup>1</sup>, Fabio Nardecchia<sup>2</sup>, Elena Conigliaro<sup>1</sup>, Paolo Monti<sup>1</sup>,  
Giovanni Leuzzi<sup>1</sup> and Armando Pelliccioni<sup>3</sup>*

<sup>1</sup>DICEA, University of Rome “La Sapienza”, Via Eudossiana 18, Rome. Italy.

<sup>2</sup>DAEEE, University of Rome “La Sapienza”, Via Eudossiana 18, Rome. Italy.

<sup>3</sup>INAIL-DIMEILA, Via Fontana Candida 1, 00040 Monteporzio Catone, Roma, Italy

**Abstract:** This paper presents a CFD analysis of the wind velocity simulated in a portion of the campus of the University of Rome “La Sapienza” (Italy). One of the final goals of this study is the evaluation of the pressure field on the surfaces of the buildings in order to quantify outdoor-indoor exchanges of air mass within a street canyon adjacent to the building of interest. Numerical results concerning the wind field have been compared with in situ data collected in the framework of the VIEPI (Integrated Evaluation of Indoor Particulate Exposure) project.

**Keywords:** *CFD simulations, complex urban geometry, buildings, urban flow, field measurements.*

## **INTRODUCTION**

In last decades, the increase in urbanization has dramatically changed the urban morphology and climatology. The most obvious consequences can be seen in an increase in energy consumption and gradual reduction of green areas, replaced with roads, large areas of concrete and large vertical surfaces. Locally, the presence of an urban area changes air temperature and humidity as well as the pattern and the structure of the wind regime, with complex flows within the streets and squares (Blocken et al., 2011). The interaction between atmospheric boundary layer flows and buildings have been widely investigated in recent years (Gousseau et al., 2011; Ramponi and Blocken, 2012). At the micro-scale, Computational Fluid Dynamics (CFD) has become more attractive because of its ability to simulate realistically building arrangements and complex scenarios (Buccolieri et al., 2013; Blocken et al. 2011). Particular attention has generally been focused to the relation to the urban air quality due to their importance in many aspects, like environmental science, meteorology and wind engineering (Franke et al., 2007; Garau et al., 2018; Salvati et al., 2019).

In this paper, micro-scale CFD simulations of the wind flow within a large portion (nearly 1 km<sup>2</sup>) of the Roman urban area have been carried out. The area of interest corresponds to that of the University of Rome “La Sapienza”, located in the Rome center. The study is based on grid-convergence analysis and model validation against in situ wind velocity measurements collected on the roof of one of the buildings and at two heights within an adjacent street canyon. The study is part of the VIEPI (Integrated Evaluation of Indoor Particulate Exposure) project, whose main goal is the evaluation of the infiltration factors of particulate matter in indoor environment.

## **DESCRIPTION OF THE STUDY AREA AND METEOROLOGICAL CAMPAIGNS**

The area of interest corresponds to the campus of University of Rome “La Sapienza”. It is located in the center of Rome, with several avenues and intersections heavily trafficked, especially at rush hours. This district is morphologically heterogeneous, with vegetation, buildings of different heights and complex geometry, heavily trafficked streets, high presence of pedestrians and crossings of primary importance for the city (Figure 1a). The diurnal cycle of winds in Rome has a main contribution from land-sea breezes (Leuzzi and Monti, 1997; Petenko et al., 2011), involving flows with complex pattern and high levels of air pollution (Monti and Leuzzi, 2005). Different experimental campaigns were carried out in this area during 2018 in the framework of the VIEPI project. In particular, three sonic anemometers were located

near the most interesting building (blue star in Figure 1a): the first is located at the roof of the building at about 28.5 m above ground level (AGL), while the remaining two are positioned within the adjacent street canyon at 7 and 16 m AGL, respectively. The two anemometers located in the street canyon are placed 0.80 m off the wall of the building (yellow dot in Figure 1a). In this study, the focus is on 21 April 2018. Two different simulations were carried out in order to simulate both daytime (14 UTC) and nighttime (01 UTC) situations.

### PHYSICAL MODEL AND GEOMETRY

The CFD software ANSYS Fluent 18.0.0 (Fluent Ansys Inc., 2006) is used for the present work. The CFD model used for the simulations is a Standard  $k-\varepsilon$  turbulence closure based on the 3D Reynolds-Averaged Navier-Stokes (RANS) equations. Boussinesq's approach is considered, solving also the energy equation. A radiation model is implemented in the model in order to take into account the heat fluxes. The Standard  $k-\varepsilon$  turbulence closure assures good performance for the analysis of the turbulence within urban canopies (Franke et al., 2004). Pressure-velocity coupling is carried out using the PISO scheme; pressure interpolation is standard, while momentum, turbulent kinetic energy, turbulent dissipation rate and energy are discretized using the second order scheme (Cannata et al., 2015). For the purpose of this work, only a portion of the campus is considered (Figure 1b). The computational domain and grid are defined according to the guidelines by Franke et al. (2007) and Tominaga et al. (2008): the upstream, downstream and lateral length of the domain is  $15 H_b$ , while the vertical extension of the domain is  $10 H_{max}$ . Here,  $H_b=25$  m is the height of the investigated building (i.e. the building where the in situ measurements are carried out) and  $H_{max}=35$  m is the maximum height of the buildings. Hence, the resulting numerical domain is  $1297 \times 1345 \times 350$  m<sup>3</sup>. ANSYS Modeler is used for the mesh discretization. The cells size varies from 0.25 m close to the ground and the buildings up to 25 m at the external boundaries of the domain. In order to minimize the transition between the small cells and the larger cells near the outer walls of the domain, two subdomains are created (Figure 1b). Preliminarily, a sensitivity test is carried out to choice the correct dimensions of the grid, comparing results obtained with three different grids (Table 1). Simulations have been performed using mesh B, which converges naturally. Hexahedral cells have been adopted in all the considered cases.

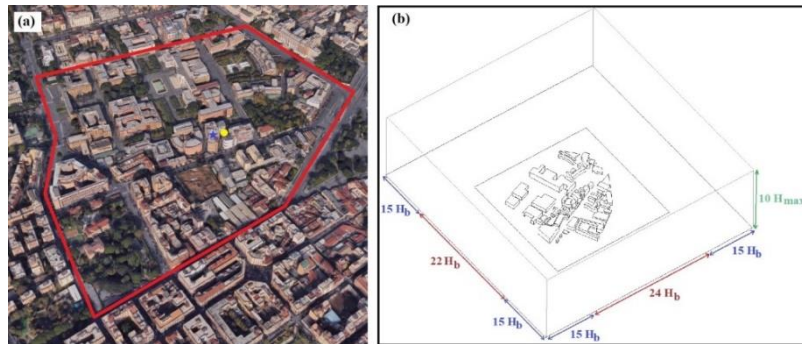


**Figure 1:** (a) Aerial view of the campus of University of Rome “La Sapienza”. The red line represents the modeled built area; the blue star identifies the building of interest and the yellow dot corresponds to the vertical where the anemometers used for comparison are located. (b) Computational domain.

**Table 1:** Characteristics of the three meshes used for the grid independence test and corresponding percentage differences  $\Delta$ .

	<b>Mesh A</b>	<b>Mesh B</b>	<b>Mesh C</b>
Number of cells	$\approx 1.6 \cdot 10^6$	$\approx 2.5 \cdot 10^6$	$\approx 4.7 \cdot 10^6$
Mesh interval size (m)	3 - 30	0.25 - 25	1.5 - 20
$\Delta$ (%)	5.91	-	0.56

### BOUNDARY CONDITIONS

Depending on the flow direction, a flow boundary condition as either velocity inlet or outflow is imposed on each external face of the domain. In particular, in every simulation, two faces are considered as velocity inlet and the remaining two as outflow. At the inlets, a logarithmic wind velocity profile  $U(z)$  is imposed:

$$U(z) = \frac{u_*}{k} \ln\left(\frac{z}{z_0}\right) \quad (1)$$

where,  $u_*$  is the friction velocity,  $k=0.41$  is the von Karman constant and  $z_0=0.1$  m is the aerodynamic roughness length. The reference wind speed at  $z=10$  m and direction used for the calculation of the logarithmic profile are obtained from the meteorological station located at G.B. Pastine airport in Ciampino, thereabout 10 km southeast of Rome. Ciampino meteorological station also provided the spatially constant air temperature imposed at the inlets. The ground of the domain is modeled as a free-slip wall, which assumes zero normal gradients for all the variables providing the physical properties of the asphalt. The top of the computational domain is modeled as a free-slip wall, too. For the daytime simulations, solar radiation is considered, while the effect of anthropogenic heat sources has been neglected. The solar calculator, implemented in ANSYS Fluent, allows the identification of the sun direction vector and the diffuse portion of the total radiation coming to the surface using the sun position at any time of the day during the year. The absorption of the radiative heat by the surfaces depends on the absorptivity values provided for each material, while heat storage by the solid regions is computed based on the specific thermal diffusivity. All simulations are performed setting the residual to  $10^{-6}$  for the three velocity components, continuity equation, energy equation, turbulent kinetic equation and  $10^{-3}$  for  $\epsilon$ .

## RESULTS

Two different simulations have been performed in order to better analyze differences in flow pattern with different anemological situations. On 21<sup>th</sup> April 2018 at 14 UTC the wind blew, according to the sea-breeze regime of this region, from southwest. Figure 2a shows the horizontal contour map of the wind speed at  $z=28.5$  m AGL, i.e. at the height of the anemometer installed on the roof of the building of interest.

After identifying the point of the computational domain corresponding to the measurement stations, the vertical planes passing through the anemometer in the directions parallel and perpendicular to the building wall are provided. This analysis allows the evaluation of the flow incident on the walls and windows of the building. Figures 2b and 2c show examples of the velocity magnitude field along the vertical planes parallel and perpendicular to the wall of the building of interest, respectively.

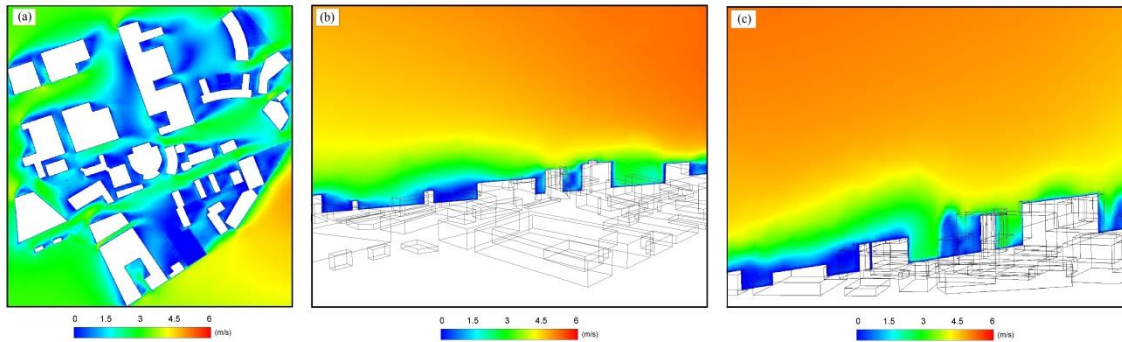


**Figure 2:** (a) Horizontal field of wind velocity at 28.5 m AGL. (b) Wind velocity magnitude in the vertical plane parallel and (c) perpendicular to the building wall. Fields are referred to 21<sup>th</sup> April 2018 at 14 UTC.

As shown in Table 2, the CFD model provides quite correct results in comparison with the anemometer placed on the roof of the building (error less than 8% in each component), while the error increases by comparing the results with the data measured within the street canyon adjacent to the building. In particular, the model does not capture the direction of meridional component of the wind. The large error that emerges from the comparison with the anemometers placed within the canyon shows that, even if the mesh has been refined near the wall, the simulation can not capture the small-scale phenomena such as vortices and turbulent structures. A similar analysis was also carried out in the nighttime case. In this case, because of the presence of the land breeze, the wind blows from North East. In Figure 3a, the horizontal field of wind speed at 28.5 m AGL is shown, while the vertical velocity fields are shown in the

direction parallel (Figure 3b) and perpendicular (Figure 3c) to the building wall, already shown for the daytime case.

**Table 2:** Comparison between CFD results and observations collected by the three anemometers on 21<sup>th</sup> April 2018 at 14 UTC. *u*, *v* and *w* represent the zonal, meridional and vertical components of the wind velocity, respectively.

		<i>u</i> (m/s)	<i>v</i> (m/s)	<i>w</i> (m/s)
z=7 m AGL	CFD	-0.0831	0.2713	1.0229
	Observations	-0.1014	-0.1907	0.4138
	$\Delta$	0.0183	0.4620	0.6091
z=16 m AGL	CFD	-0.0516	0.6526	0.6623
	Observations	-0.0519	0.0380	0.4302
	$\Delta$	0.0003	0.6146	0.2320
z = 28.5 m AGL	CFD	2.8323	2.2011	0.3888
	Observations	3.0376	2.3423	0.3726
	$\Delta$	0.2053	0.1412	0.0162

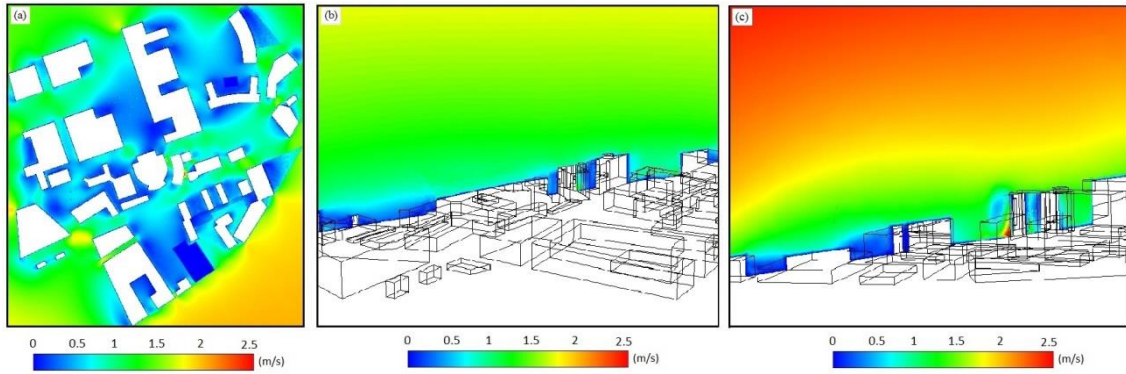


**Figure 3:** (a) Horizontal field of wind velocity at 28.5 m AGL. (b) Wind velocity magnitude in the vertical plane parallel and (c) perpendicular to the building wall. All cases refer to 21<sup>th</sup> April 2018 at 03 UTC.

**Table 3:** Comparison between CFD results and observations collected by the three anemometers on 21<sup>th</sup> April 2018 at 03 UTC. *u*, *v* and *w* represent the zonal, meridional and vertical components of the wind velocity, respectively.

		<i>u</i> (m/s)	<i>v</i> (m/s)	<i>w</i> (m/s)
z=7 m AGL	CFD	0.0344	-1.3620	-0.0551
	Observations	0.3842	0.3823	0.0685
	$\Delta$	0.3498	1.7443	0.1236
z=16 m AGL	CFD	0.0192	-0.3525	-0.2297
	Observations	-0.1825	-0.2370	0.5674
	$\Delta$	0.2017	0.1155	0.7971
z=28.5 m AGL	CFD	-0.7757	-0.8629	-0.0095
	Observations	-0.8811	-0.9596	0.0477
	$\Delta$	0.1054	0.0967	0.0572

In the nighttime simulation, the wind velocity near the ground is lower than 2.5 m/s. In particular, close to the building of interest, the typical canyon effect can be observed. The wind, blowing from North East, channeled between buildings and the velocity increases at the center of the domain, i.e. in the canyon where the anemometers are located (Figure 3c). The point analysis shown in Table 3 highlights this phenomenon; in fact, the meridional (i.e. the component almost parallel to the street canyon) component of the velocity shows high values, especially near the ground. This effect decreases as the height increases. Consequently, the comparison with measurements gives good agreement above the rooftop while, within the canyon, the error increases.

## CONCLUSIONS

The goal of this work was the analysis of the flow characteristics in a portion of a campus by means of

CFD simulations. Numerical results have been compared to field measurements carried out near the building of interest. To investigate the influence of meteorological condition on the flow patterns in the area, two anemological situations were studied. The daytime simulation (21<sup>th</sup> April 2018, 14 UTC) has provided results in agreement with field measurement. In the nighttime case (21<sup>th</sup> April 2018, 03 UTC), differences between numerical results and measurements are more evident and larger errors occur. These results must be seen as preliminary tests. In fact, more accurate simulations are needed to better reproduce the flow, especially within the canyons, where the high complexity of the geometry involves the formation of complex structures that are not correctly reproduced in the present work.

#### ACKNOWLEDGEMENTS

This research was supported by the BRiC (ID 22) fund from INAIL (Project VIEPI: “Integrated evaluation of particulate pollutant for indoor air quality”).

#### REFERENCES

- Blocken, B., T. Stathopoulos, J. Carmeliet and L. M. Hensen, 2011: Application of computational fluid dynamics in building performance simulation for the outdoor environment: an overview. *J. Build. Perform. Simu.*, **4**, 157-184.
- Blocken B., W. D. Janssen and T. van Hooff, 2011: CFD simulation for pedestrian wind comfort and wind safety in urban areas: General decision framework and case study for the Eindhoven University campus. *Environ. Model. Softw.*, **30**, 15-34.
- Buccolieri, R., F. Sartoretto, A. Giacometti, S. Di Sabatino, L. Leo, B. Pulvirenti and H. Wigö, 2010: Flow and pollutant dispersion within the Canal Grande channel in Venice (Italy) via CFD techniques. *13th International Conference on Harmonisation within Atmospheric Dispersion Modelling for Regulatory Purposes, HARMO 2010, 1-4 June 2010, Paris, France* (pp. 760-764).
- Cannata, G., F. Lasaponara and F. Gallerano, 2015: Non-linear Shallow Water Equations numerical integration on curvilinear boundary-conforming grids. *WSEAS Transactions on Fluid Mechanics*, **10**, 13-25.
- Fluent Inc., 2006. Fluent 6.3 User’s Guide. Fluent Inc., Lebanon.
- Franke, J., A. Hellsten, H. Schlünzen and B. Carissimo, 2007: Best practice guideline for the CFD simulation of flows in the urban environment. COST Action 732, Quality Assurance and Improvement of Meteorological Models.
- Gallerano, F., G. Cannata, F. Lasaponara, and C. Petrelli, 2017: A new three-dimensional finite-volume non-hydrostatic shock-capturing model for free surface flow. *J. Hydrodyn.*, **29**, 552-566.
- Garau, M., M.G. Badas, S. Ferrari, et al. (2018) Turbulence and Air Exchange in a Two-Dimensional Urban Street Canyon Between Gable Roof Buildings. *Boundary-Layer Meteorol.*, **167**, 123–143.
- Gousseau P., B. Blocken, T. Stathopoulos, G. J. F. van Heijst, 2011: CFD simulation of near-field pollutant dispersion on a high-resolution grid: A case study by LES and RANS for a building group in downtown Montreal. *Atmos. Environ.*, **45**, 428-438.
- Leuzzi, G. and P. Monti, 1997: Breeze Analysis By Mast and Sodar Measurements. *Nuovo Cimento C*, **20**, 343-359.
- Monti, P. and G. Leuzzi, 2005: A numerical study of mesoscale airflow and dispersion over coastal complex terrain. *Int. J. Environ. Pollut.*, **25**, 239–250.
- Pelliccioni, A., P. Monti and G. Leuzzi, 2016: Wind-speed profile and roughness sublayer depth modelling in urban boundary layers. *Boundary-Layer Meteorol.*, **160**, 225-248.
- Petenko, I., G. Mastrantonio, A. Viola, S. Argentini, L. Coniglio, P. Monti and G. Leuzzi, 2011: Local circulation diurnal patterns and their relationship with large-scale flows in a coastal area of the Tyrrhenian Sea. *Boundary-Layer Meteorol.*, **139**, 353-366.
- Ramponi, R. and B. Blocken, 2012: A computational study on the influence of Urban morphology on wind-induced outdoor ventilation. *Proceedings of the 6th Biennial Meeting of the International Environmental Modelling and Software Society*, pp. 2693-2700.
- Salvati, A., P. Monti, H. Coch Roura and C. Cecere, 2019: Climatic performance of urban textures: analysis tools for a Mediterranean urban context. *Ener. Build.*, **185**, 162–179.
- Tominaga, Y., A. Mochida, R. Yoshie, H. Kataoka, T. Nozu, M. Yoshikawa and T. Shirasawa, 2006: AIJ guidelines for practical applications of CFD to pedestrian wind environment around buildings. *J. Wind. Eng. Ind. Aerod.*, **96**, 1749-1761.